

A Sustainable and User Behavior Aware Cyber-Physical System for Home Energy Management

WEI LI, The University of Sydney, Australia

XIAOMIN CHANG, The University of Sydney, Australia

JUNWEI CAO, Tsinghua University, China

TING YANG, Tianjin University, China

YAOJIE SUN, Fudan University, China

ALBERT Y. ZOMAYA, The University of Sydney, Australia

There is a growing trend for employing cyber-physical systems to help smart homes to improve the comfort of residents. However, a residential cyber-physical system is differed from a common cyber-physical system since it directly involves human interaction, which is full of uncertainty. The existing solutions could be effective for performance enhancement in some cases when no inherent and dominant human factors are involved. Besides, The rapidly rising interest in the deployments of cyber-physical systems at home does not normally integrate with energy management schemes, which is a central issue that smart homes have to face. In this paper, we propose a cyber-physical system based energy management framework to enable a sustainable edge computing paradigm while meeting the needs of home energy management and residents. This framework aims to enable the full use of renewable energy while reducing electricity bills for households. A prototype system was implemented using real world hardware. The experiment results demonstrated that renewable energy is fully capable of supporting the reliable running of home appliances most of the time and electricity bills could be cut by up to 60% when our proposed framework was employed.

CCS Concepts: • **Computer systems organization** → **Embedded systems**; *Redundancy*; Robotics; • **Networks** → Network reliability;

Additional Key Words and Phrases: cyber-physical system, human interaction, scheduling, energy management, renewable energy

ACM Reference Format:

Wei Li, Xiaomin Chang, Junwei Cao, Ting Yang, Yaojie Sun, and Albert Y. Zomaya. 2018. A Sustainable and User Behavior Aware Cyber-Physical System for Home Energy Management. *ACM Comput. Entertain.* 9, 4, Article 39 (March 2018), 21 pages. <https://doi.org/0000001.0000001>

Authors' addresses: Wei Li, Centre for Distributed and High Performance Computing, School of Information Technologies, The University of Sydney, J12/1 Cleveland St, Darlington, NSW, 2008, Australia, weiwilson.li@sydney.edu.au; Xiaomin Chang, The University of Sydney, J12/1 Cleveland St, Darlington, NSW, 2008, Australia, cha8737@uni.sydney.edu.au; Junwei Cao, Tsinghua University, Beijing, China, jcao@mail.tsinghua.edu.cn; Ting Yang, Tianjin University, Tianjin, China, yangting@tju.edu.cn; Yaojie Sun, Fudan University, Shanghai, China, yjsun@fudan.edu.cn; Albert Y. Zomaya, The University of Sydney, J12/1 Cleveland St, Darlington, NSW, 2008, Australia, albert.zomaya@sydney.edu.au.

Permission to make digital or hard copies of all or part of this work for personal or classroom use is granted without fee provided that copies are not made or distributed for profit or commercial advantage and that copies bear this notice and the full citation on the first page. Copyrights for components of this work owned by others than ACM must be honored. Abstracting with credit is permitted. To copy otherwise, or republish, to post on servers or to redistribute to lists, requires prior specific permission and/or a fee. Request permissions from permissions@acm.org.

© 2018 Association for Computing Machinery.

Manuscript submitted to ACM

Manuscript submitted to ACM

1 INTRODUCTION

A cyber-physical system (CPS) is a system of systems to allow physical phenomena to be probed or controlled via information-based approaches. The system generally includes processing modules that are responsible for acquiring data from sensors in a timely manner and issuing commands to operate actuators meet user needs. In recent years, CPS applications can be found on a wide spectrum of daily activities, including but not limited to home automation, smart grid, healthcare, vehicular applications and smart cities. Despite the primary purpose of the design of such a system being to enable bidirectional object-object interactions, human-object interactions are increasingly integrated into the expanding apparatus of the applications. With the involvement of human activities and interactions, expanded CPS (human-in-the-loop CPS, or HilCPS) would offer a great opportunity for restoring or augmenting human interaction with the physical world [Schirner et al. 2013].

As a popular CPS application associated with significant human interactions, smart home introduces enhanced monitoring and control functionality into residential environments. The energy consumption of households is always a noticeable issue since it accounts for around 35% of the overall consumption of all activities [Venkatesh et al. 2013]. Multiple studies have shown that residential energy consumption can be effectively reduced by dynamically adjusting the power demands of home appliances and electric vehicles. For example, the use of CPS-based home energy systems [Zhou et al. 2016] has successfully helped residents to reduce their electricity bills by shifting loads from peak hours to non-peak hours. However, the dual characteristics of regularity and variability of residents' behaviors could degrade the performance of most existing solutions when the human factor is not fully addressed. It is also vital to determine the willingness of residents to change their behaviors in cooperation with the energy management schemes without affecting their daily activities. Otherwise, the potential benefits gained from those energy management schemes may not be able to deliver as promised. It is also important to note that a significant portion (over 80%) of today's energy is still generated by fossil fuels (brown energy) [Eco [n. d.]]. As is well known, the widespread use of fossil fuels is implicated in global climate warming. Carbon taxes have helped to reduce the rapid anthropogenic release of carbon dioxide from fossil fuel, but also to drive up electricity prices for residents. To effectively lower the electricity bill in a sustainable way, the employment of renewable energy (green energy) is equally important to reduce the total energy demand of households from utility grid. With the growth of distributed power generators, they are capable of powering an increasing number of residents from green energy sources. Typical examples of these small on-site energy generators include rooftop solar panels, microturbines, and micro-wind generators. Advanced energy storage, e.g. thin-film batteries and super-capacitors, have become more mature and are usually used in combination with these green energy sources to better utilize them. These technologies open a new avenue for supporting various applications of smart homes.

In this article, we propose a framework design by integrating multiple renewable energy sources with smart homes to form a HilCPS environment in households by explicitly considering the human factor so as to reduce the electricity bill efficiently while still meeting the needs of the residents. In this design, we developed a smart appliance scheduling-based approach to manage residential energy based on user behavior constraints. These behavior constraints are represented by user willingness, which is formally modelled as the flexibility of the residents using different appliances. We adopted an information theory approach to analyze the cumulative distribution functions (CDF) of the starting time of various types of smart appliances. To obtain a quantitative measure, the entropy value of a CDF is used to indicate how a given appliance can be used, e.g. no flexibility, 1h-3h flexibility, etc. With these deadline values, we can treat the use of smart appliances as automatic jobs that can be scheduled to use the energy resource. We convert flexibility into deadlines and

105 then assign reasonable deadlines to different appliance in different households and the underlying assumptions on user
106 behaviors can be eliminated. In addition to that, we integrate with load determination and scheduling techniques to
107 maximize the use of renewable energy harvesting from the ambient environment to minimize the electricity cost to a
108 household. Our framework is able to achieve 75% energy savings and cut 60% from the electricity bill in a household,
109 compared to the case where no such appliance scheduling is deployed.
110
111

112 2 RELATED WORK

113 Cyber-physical systems have been widely studied in the past and extensively used in industrial applications. Recently,
114 researchers have started paying attention to investigating the interactions between human beings and CPS systems.
115 In [Schirner et al. 2013], the human-in-the-loop CPS (HilCPS) is introduced as a specific type of CPS to denote the
116 CPS systems that are involved with human factors. HilCPS is increasingly used in multiple domains, e.g. residential
117 applications [Aksanli and Rosing 2017] and healthcare applications [Nunes et al. 2015].
118
119

120 One of the residential applications of HilCPS is to manage the energy consumption of home appliances based on
121 the study of the historical activities of users. To extract the behavior patterns from residents, multiple approaches
122 were developed accordingly to achieve the same goal. In [Cottone et al. 2015], [Muratori et al. 2013], the authors used
123 common available activity data sets to group the users' behavior into different categories based on multiple criteria, e.g.
124 age, gender, head counts in a house and employment status. With the help of these datasets, the researchers can either
125 determine the sequences of a set of activities by using machine learning approach [Keshtkar and Arzanpour 2017], or
126 which activity is most likely related to what appliance in a household [Delzende et al. 2017]. After that, the starting
127 time of a given appliance and its operating conditions can be further estimated. The overall energy consumption of a
128 household is then simply summed up on all the appliances. The major issue of this type of approach is that no realtime
129 information about users can be obtained so that it becomes an offline design. Other studies collect the behavior of users
130 directly. In [Yin et al. 2016], the user behavior is defined as the user's preference. In [Lee et al. 2013], user behavior is
131 extensively studied in considering their willingness to use appliances. However, in this study the factor of flexibility
132 was not addressed and the privacy concern was triggered since it is necessary to collect personal profiles from smart
133 phone. By far, only a few studies [Aksanli and Rosing 2017], [Zhai et al. 2018] have conducted quantitative analysis
134 on the flexibility of appliances. Most of those approaches just utilize the power consumption of smart appliances.
135 Besides, controllability is usually only considered for energy hungry appliances, e.g. HAVC (Heating, Ventilation and
136 Air Conditioning) and electric vehicles (EV). In addition, both existing research work and developed home energy
137 management systems (HEMS) rarely address the integration of sustainable energy.
138
139
140
141
142

143 In an effort to address the issue of using sustainable energy to support the running of HEMS, we propose a low-cost
144 sustainable HilCPS design as a home-level extension of the exploratory design of our sustainable edge computing
145 systems [Li et al. 2018], which can not just reduce the electricity tariff, but also meet the needs of smart home applications
146 and home energy management. In our HilCPS, the physical devices are the appliances and the sensing devices that
147 provide the essential information, the cyber part is the appliance management functionalities running on the portable
148 computing device and the residents frequently interact with the physical devices during their daily routines.
149
150

151 3 SYSTEM DESIGN OUTLINE

152 This section illustrates the HilCPS-based energy management framework for home appliances. We first introduce the
153 overall design of the system. Then we provide the details of the function of the system modules and the interactions
154 between them.
155
156

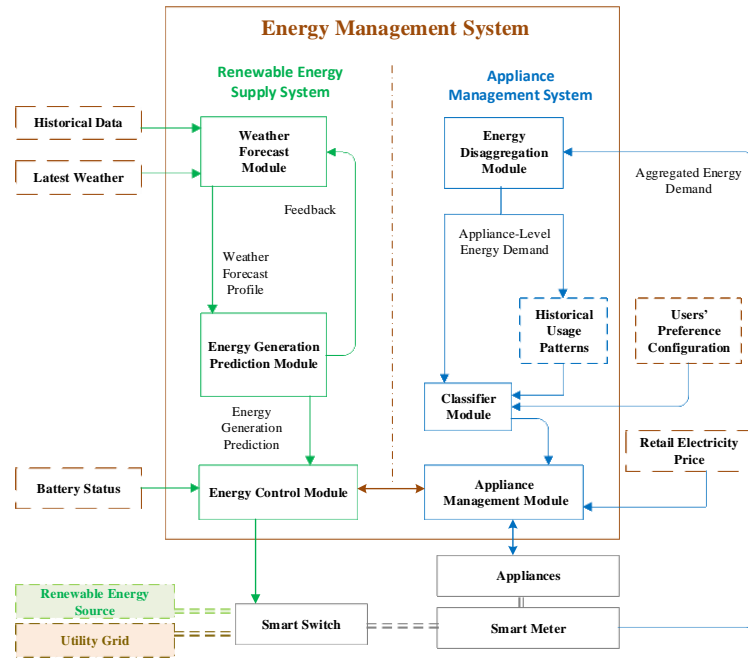


Fig. 1. The System Framework

3.1 System Overview

The proposal of our energy management system is designed for greening smart appliances, which aims to maximize the use of renewable energy in ordinary households while still conforming to users' needs. The overview of our design is depicted in Fig. 1, which contains two sub-systems, namely renewable energy supply system and appliance management system. With such a design, the operation time of smart appliances is automatically scheduled based on users' preferences, day-ahead electricity price, and historical usage profiles. Meanwhile, the system takes advantage of renewable energy harvesting techniques, the converted and stored renewable energy are used to minimize energy consumption from the utility grid in peak hours.

The renewable energy supply sub-system aims to maximize renewable energy utilization with an optimal energy allocation scheme. The major challenge of the sub-system is the intermittency of renewable energy generation, which is caused by the fluctuation of sunlight intensity. To address this issue, the sub-system integrates three modules with the functions of weather forecast, energy generation prediction and renewable energy management respectively. Receding horizon control strategy [Mattingley et al. 2011] is used for both the forecasting module and the renewable energy management module to achieve optimal renewable energy allocation.

The appliance management sub-system aims to minimize drawing electricity from the utility grid, particularly in peak hours when the energy price is high. In this sub-system, a smart meter is used to collect the overall load of a household and pass it to the energy disaggregation module. The voltage and current of individual appliances can be derived from the overall load in the energy disaggregation module. By analyzing the changes in current, the energy disaggregation module provides the real-time status of each appliance in the household. Then the appliance-level energy

209 demand is passed to the classifier module, where the appliances are classified by users' preference profiles and historical
210 usage records of appliances. The classifier filters the operating requests of appliances according to user requirements
211 and the features of the appliances, only the selected information is passed to the appliance control module. In the
212 appliance control module, the operation time of appliances is scheduled in order to maximize utilization of renewable
213 energy.
214
215

216 3.2 System Components

217 **Weather forecast module:** The weather forecast module is responsible for providing coefficients associated with
218 renewable energy generation, e.g. sunlight intensity, wind intensity, temperature and global horizontal irradiance. At
219 the initial stage, the weather forecast module loads historical data that includes location information and day-ahead
220 historical weather data. Then a weather forecast is generated based on the initial inputs. However, the uncertainty
221 of cloud has a significant impact on renewable energy generation. It is hard to predict the formation, movement and
222 dissipation of cloud only based on historical data. To reduce the deviation from the weather forecast module, a receding
223 horizon control strategy is adopted in this module. The weather forecast is repeatedly computed on a pre-defined time
224 granularity with the latest information, and the latest result will then be passed to the energy generation prediction
225 module for further processing.
226
227
228

229 **Energy generation prediction module:** In this module, the output of renewable energy harvesting is estimated
230 by the inputs from the weather forecast module and the hardware specifications of the renewable energy generator.
231 For example, solar energy is a common type of renewable energy source. As is well known, the power generation of a
232 solar panel is based on the volt-ampere characteristics of solar cells. In open-circuit solar cells, voltage decreases with
233 temperature rise while other factors remain constant [Cuce et al. 2013]. Thus, with the prediction weather profile and
234 renewable energy generator properties, energy generation from renewable energy sources can be predicted accordingly.
235 Then the result is passed to the energy control module.
236
237

238 **Energy control module:** In the energy control module, there are three input profiles, including battery status,
239 real-time energy demand and energy generation prediction. In this module, we aim to maximize the utilization of
240 renewable energy by reducing conversion loss from charging and discharging batteries. Electricity from the renewable
241 power system is given priority over the utility grid, with the surplus renewable energy stored in batteries. In our system
242 design, smart appliances can be purely powered by either renewable power system or utility grid. A smart switch is
243 equipped to connect both types of energy sources but only draws power from one source in any given time period.
244

245 **Energy disaggregation module:** Before stepping into appliance scheduling, our proposed system needs to be
246 aware of historical details of execution time of each appliance for deducing user activities on a typical day. Based on
247 this fine-grained appliance-level information, usage patterns of each appliance can also be derived and given a high
248 priority so that the schedule plan generated from the appliance control module will retain a resemblance of customers'
249 daily routines. Hence, for getting appropriate scheduling strategies for a household, usage patterns and features of each
250 appliance are key information in need of timely acquisition as inputs. In general, Appliance Load Monitoring (ALM)
251 approaches [Hosseini et al. 2017] can be employed to obtain this information. ALM approaches can be divided into
252 two types, namely Intrusive Load Monitoring (ILM) and non-Intrusive Load Monitoring (NILM). For ILM, tremendous
253 numbers of metering devices and sensors are deployed to achieve energy monitoring on each appliance in a distributed
254 way, which leads to high cost of capital investment and increases complexity of system installation and maintenance.
255 In contrast, NILM techniques have gained increasing popularity in both research and industry in recent years, and
256 conduct energy disaggregation only based on overall energy consumption [Giri and Bergés 2015]. Advanced NILM
257
258
259
260

261 techniques can be categorized into supervised NILM and unsupervised NILM. Most supervised NILM algorithms need
262 extensive data sets for training and modeling of each appliance, which is hard to retrieve for household scenarios. As
263 for the unsupervised NILM algorithms, like factorial hidden Markov models and artificial neural networks, they are
264 computationally intensive. Considering these factors, a location-aware NILM approach [Uttama Nambi et al. 2015] is
265 employed in our design, which not only reduces the complexity of computation, but also requires much less historical
266 data for appliance modeling.
267

268 **Classifier module:** This module is designed for classifying the smart appliances into shiftable and unshiftable,
269 and passing the information of shiftable appliances with adjustable range to the next module. The purpose of such
270 classification is to satisfy householders' needs while completing the rescheduling of the appliances. The classification
271 process is mainly based on flexibility. Flexibility refers to the extent to which the start time of an appliance can be
272 adjusted, which depends on distribution of appliance usage during a day. Appliances with uniform usage distribution
273 have better flexibility than those appliances that are always used around a certain preferable usage period. For example,
274 lighting is a kind of rigid demand so that lamps theoretically have low flexibility. In contrast, dish washers might have
275 higher flexibility as people are normally not in rush with those demands. Unshiftable appliances with low flexibility
276 can be scheduled to another time only with difficulty. Thus, in our design, the system only reschedules the running of
277 shiftable appliances with high flexibility.
278
279

280 To quantitatively obtain the flexibility of each appliance, we used an approach similar to that in [Aksanli and Rosing
281 2017] to modeling user flexibility. Based on historical data derived from the energy disaggregation module, the start
282 times of each appliance are first extracted. Then we plot the graph of cumulative probability density function (CDF)
283 for start times of each appliance, which presents the load distribution of a specific appliance and its usage patterns.
284 After that, each CDF graph is assigned with an entropy value between 0 to 5. Each entropy value is associated with a
285 threshold of time period to be adjusted, during which the start time of a given appliance job can be shifted accordingly.
286 Each threshold not only reflects the flexibility of an appliance, but also determines job deadline. On the other hand,
287 correlation is another coefficient to be considered during the scheduling process to satisfy user demands. It indicates
288 the associations between different appliances, such as relevance and execution order. For example, radiant-cooker and
289 range hood are usually used together. At the initial stage, the classifier module generates a preset user preference profile
290 based on the variety of appliance and historical records. But householders are able to modify the profile at all times to
291 better conform to their own habits.
292
293
294
295

296 In addition, appliances can be further classified into adjustable and unadjustable, which is based on user preferences.
297 For an adjustable appliance, the setpoints or working mode can be dynamically altered based on user preferences.
298 An unadjustable appliance always works in a fixed mode. Different to flexibility, user preference profiles can be set
299 manually based on the personal habit of each resident.
300

301 **Appliances management module:** This module plays a vital role in this system, which is mainly responsible for
302 job allocation and online scheduling. Once an appliance job is released, it will be allocated in an appropriate queue based
303 on the allocation algorithm presented in Section 5. Thus, the energy source for powering the running of this appliance
304 can be determined. After that, online scheduling will be achieved by employing the scheduling strategies in Section 5.
305 During this process, the permutation as well as the energy source for jobs could be adjusted to guarantee system-level
306 and appliance-level requirements. On the other hand, the start time of each job within the corresponding queue can
307 also be shifted. Based on the profile from the classifier module, the type of any given appliance can be identified. For
308 jobs released by unshiftable appliances, this module cannot change its start time. Instead, the start time of the jobs
309 released by shiftable appliances can be adjusted within the corresponding threshold period obtained from the classifier
310
311

Table 1. Key Parameters

Notation	Definition
α	Appliances set in a household.
α_{shift}	A set of shiftable appliances.
$\alpha_{unshift}$	A set of unshiftable appliances.
α_i	The i th element in the set α (for short, we use α_i to denote as an appliance from now on).
η^d	The number of total appliances in a household.
$P_{\alpha_i}^{max}$	Maximum power consumption of an appliance α_i .
$P_{\alpha_i}(t)$	The real-time power consumption of appliance α_i at operation time t .
T_{α_i}	Maximum tolerance duration of a particular job released by appliance α_i .
L_{α_i}	Maximum operation time for appliance α_i to finish a particular job.
m_{α_i}	A set of working modes or setpoints of appliance α_i .
ρ_{α_i}	A set of values of power consumption, each of which matches up to a particular working mode of appliance α_i .
ω_{α_i}	A set of possible performance impacts made by appliance α_i .
ψ	A set of renewable energy sources used in household environment to generate electricity.
η^s	The number of renewable energy sources in the set ψ .
ψ_i	The i th element in ψ .
$P_{\psi_i}(t)$	Power generation from renewable energy source ψ_i at time t .
$P_{\psi_i}^{max}(t)$	Maximum total output power from each renewable energy source at time t .
$P_{\psi_i}^d(t)$	Actual output power supplied to appliances at time t .
p_c^{min}	Minimum charging power of the battery.
p_c^{max}	Maximum charging power of the battery.
p_d^{max}	Maximum discharging power of the battery.
$P_c(t)$	Actual charging power at time t .
$P_d(t)$	Actual discharging power at time t .
E_{max}	Battery capacity, representing the maximum amount of energy that can be stored in the battery.
$P_{loss}(t)$	Power dissipation on battery at time t .
$P_{grid}(t)$	Actual supplied power from utility grid at time t .
p_{grid}^{max}	Maximum supplied power from utility grid.
$C_{grid}(t)$	Real-time electricity price at time t .
λ_{α_k}	Appliance job released by appliance α_k .
$t_{\alpha_k}^r$	Release time of the job λ_{α_k} .
$t_{\alpha_k}^l$	Latest start time of the job λ_{α_k} .
σ	The smallest time unit.
ξ	The smallest power unit.
$Q_{release}$	A queue containing appliance jobs newly released by corresponding appliances.
Q_{ready}^r	A queue containing appliance jobs ready to be executed and powered by renewable energy
Q_{ready}^g	A queue containing appliance jobs ready to be executed and powered by utility grid
Q_{run}^r	A job queue containing appliance jobs currently running and powered by renewable energy
Q_{run}^g	A job queue containing appliance jobs currently running and powered by utility grid

model. Besides, to minimize energy consumption of an appliance, each appliance will be set to the most energy efficient mode before starting its operation. The details of scheduling strategies will be provided in the following sections.

4 SYSTEM MODELING

In this section, we first detail the models which are used in our proposal, including power demand and power supply. Afterwards, the problem formulation is formally given to describe the core problem addressed in this paper. The notations used in the rest of the paper are also listed in Table 1.

4.1 Power Demand

We model appliances in a typical household as follows, each of which entails variant power-demand operations at different time periods during a day. In a household, there is a set of smart appliances $\alpha = \{\alpha_1, \alpha_2, \dots, \alpha_{\eta^d}\}$, where η^d denotes the number of total appliances. Each $\alpha_i \in \alpha$ can be modeled by a tuple $\{P_{\alpha_i}^{max}, T_{\alpha_i}, L_{\alpha_i}\}$, where $P_{\alpha_i}^{max}$ represents its maximum power consumption, T_{α_i} is maximum tolerant duration within which operations for a job of α_i are supposed to be finished after the job is released, and L_{α_i} denotes its maximum operation time which is less than or equal to T_{α_i} . As presented in the last section, these appliances can be categorized into two types, shiftable appliances $\alpha_{shiftable}$ and unshiftable appliances $\alpha_{unshiftable}$. The start time of a job for a shiftable appliance is flexible and can be shifted within a constrained time period only if the job can be finished before the deadline. In contrast, the start time of a job from an unshiftable appliance is fixed. Therefore, if $\alpha_i \in \alpha_{shiftable}$, $L_{\alpha_i} > T_{\alpha_i}$, whereas $L_{\alpha_i} = T_{\alpha_i}$ if $\alpha_i \in \alpha_{unshiftable}$.

Both shiftable appliances and unshiftable appliances can further be classified into two groups, adjustable appliances $\alpha_{adjustable}$ and unadjustable appliances $\alpha_{unadjustable}$. Because setpoints and working modes of adjustable appliances can be selected, another three parameters $\{m_{\alpha_i}, \rho_{\alpha_i}, \omega_{\alpha_i}\}$ are required to model appliance α_i , where $\alpha_i \in \alpha_{adjustable}$. m_{α_i} is a set of working modes or setpoints which can be set. ρ_{α_i} denotes different values of maximum power consumption and each $\rho_{\alpha_i}^j \in \rho_{\alpha_i}$ can be identified once a particular $m_{\alpha_i}^j \in m_{\alpha_i}$ is selected. ω_{α_i} represents a set of possible performance impacts when the working status of appliances is varied accordingly. Considering the dynamic nature of human behavior, it is assumed that each appliance α_i can be operated multiple times, thus for each job instance, the real-time power consumption of appliance α_i during operation period can be represented as $P_{\alpha_i}(t)$.

4.2 Power Supply

As mentioned in our proposed system architecture, we practically adopt a hybrid power-supply system comprised of three major components: (i) utility grid which is responsible for distributing electricity in a centralized manner, (ii) a set of renewable energy generators, such as rooftop renewable energy generators, microturbines, and micro-wind generators, (iii) household energy storage devices. Significantly lowering the carbon footprint of smart homes requires maximizing the utilization of renewable energy at each household. Thus we use renewable energy as the primary and brown energy from utility grid as the secondary energy supply. The specific model of this home-centric power-supply system is depicted as follows.

As we take multiple renewable energy sources into account, let $\psi = \{\psi_1, \psi_2, \dots, \psi_{\eta^s}\}$ denote a set of renewable sources, where η^s is the number of elements in this set. At time t , power generation from renewable energy source ψ_i can be represented as $P_{\psi_i}(t)$. Besides, output power from each renewable energy source at t is limited to its power bound $P_{\psi_i}^{max}(t)$, which is normally less than $P_{\psi_i}(t)$ due to energy transition loss. Let $P_{\psi_i}^d(t)$ denote actual output power satisfying appliance demand. Considering uncertain nature of renewable energy, reliable forecasting techniques are supposed to be employed as means to obtain the power generation of each energy source at different time period.

In the case of $P_{\psi_i}^d(t) < P_{\psi_i}^{max}(t)$, surplus supplied power from renewable energy sources will be distributed to the energy storage device for further employment in peak hours. The use of storage in conjunction with renewable energy

sources is helpful to optimize the cost effectiveness of smart homes. Based on characteristics of the energy storage device, such as lithium-ion battery, the device is modeled with minimum charging power P_c^{min} , maximum charging power P_c^{max} , maximum discharging power P_d^{max} , battery capacity E_{max} . Let $P_d(t)$ and $P_c(t)$ denote the actual discharging power and charging power respectively, $E(t)$ is the actual battery status showing energy left. Due to the fact that there is always power dissipation $P_{loss}(t)$ on battery during the power supply at t , we need to improve utilization of energy accommodated in the battery by reducing the energy dissipated by internal resistance. According to the extensive study of the battery model by [Hredzak et al. 2014], the reduction of current could potentially reduce energy loss and extend the time for power supply.

With respect to electricity from utility grid, let $P_{grid}(t)$ denote the actual supplied power which is limited to the power bound P_{grid}^{max} . Rather than sporadic powering method of renewable energy sources, utility grid can provide stable supplied power at any time period, thus the supplied power only varies along with power demand from customers. Besides, the electricity price at time t is represented as $C_{grid}(t)$ varying constantly in accordance to real-time price adjustment from utility.

4.3 Problem Statement

The major problem for advanced energy management is defined as follows:

$$\max \frac{\int_0^T \left[\sum_{\psi_i \in \psi} P_{\psi_i}^d(t) + P_c(t) \right] dt}{\int_0^T \sum_{\psi_i \in \psi} P_{\psi_i}(t) dt} \quad (1)$$

subject to

$$\sum_{\alpha_i \in \alpha} P_{\alpha_i}(t) - P_{grid}(t) = \sum_{\psi_i \in \psi} P_{\psi_i}^d(t) \quad (2)$$

$$\sum_{\psi_i \in \psi} P_{\psi_i}^{max}(t) - \sum_{\psi_i \in \psi} P_{\psi_i}^d(t) \geq P_c(t) \quad (3)$$

$$P_{\psi_i}^d(t) \leq P_{\psi_i}^{max}(t) \quad (4)$$

$$P_c^{min} \leq P_c(t) \leq P_c^{max} \quad (5)$$

$$\int_{\Gamma}^{\Gamma+\sigma} P_c(t) dt + E(\Gamma) \leq E_{max} \quad (6)$$

$$P_{grid}(t) \leq P_{grid}^{max} \quad (7)$$

The primary objective of this work as shown in (1) is to maximize the utilization of renewable energy, which is supposed to satisfy the constraints (2), (3), (4), (5), (6), (7). $\sum_{\psi_i \in \psi} P_{\psi_i}^d(t)$ and $P_c(t)$ are control variables in objective function (1), whereas $\sum_{\psi_i \in \psi} P_{\psi_i}(t)$ is not, because renewable energy generation is mostly affected by multiple weather factors which cannot be manipulated by our system. At time t , only partial appliances releasing jobs are fully powered by renewable energy sources, and the remaining running appliances draw energy from utility grid. As shown in constraint (2), $\sum_{\psi_i \in \psi} P_{\psi_i}^d(t)$ can be identified once the number of appliances supplied by renewable energy sources is determined. To achieve it, an effective scheduling strategy is required to make a decision on selecting the energy source for each appliance. In order to balance the demand and power supply and maximize utilization of renewable energy, the start time of each shiftable appliance is supposed to be scheduled within tolerant duration T_{α_i} . Considering the constraints

(4) and (7), $P_{\psi_i}^d(t)$ for each renewable energy source ψ_i and $P_{grid}(t)$ are not supposed to exceed the corresponding power bound.

With respect to another control variable $P_c(t)$, once the total power demands $\sum_{\psi_i \in \psi} P_{\psi_i}^d(t)$ purely drawing from renewable energy and maximum output power $\sum_{\psi_i \in \psi} P_{\psi_i}^{max}(t)$ from renewable energy sources are obtained, it can be determined based on constraints (3) and (5). In order to maximize the utilization of renewable energy, surplus power is supposed to be assigned to the battery as much as possible only if the limitation on charging power is gratified. Apart from these two constraints, battery capacity is another factor that would affect decision making on the amount of power charged at time t . As shown in the constraint (6), total energy charged into battery from Γ to $\Gamma + \sigma$, where σ is the minimum arrival time unit of surplus renewable energy, also depends on the remaining energy in battery at Γ . At any time, it is expected to be guaranteed that the total energy stored in the battery cannot exceed the maximum energy capacity.

5 APPROACH AND SOLUTION

Because this energy management system resembles a quasi-real-time system, we matched the appliance scheduling problem with a real-time task scheduling problem. The two are similar, as a series of operations, contained in a job of each smart appliance, can be deemed as tasks in the applications, the deadline constraint for which is always to be satisfied. The sum of energy generation for appliance operations matches the available computing and storage resources in support of task processing. To achieve the objective presented in the last section, we first presented our designed scheduling framework for all appliance jobs in the household, and then defined appliance-level and system-level scheduling rules. This not only guaranteed meeting the deadlines for appliance operations, but also balanced the supply and demand for power. Based on these two scheduling rules, we developed three algorithms for real-time job scheduling, which was implemented across three critical stages, contained in the scheduling framework, and effectively maximized the utilization of renewable energy. In addition to the scheduling of appliance jobs, the algorithm for energy management of the battery will be presented in this section, aiming to achieve reduction of energy cost and peak demands.

5.1 Scheduling Rules

For this system, we propose appliance-level and system-level scheduling rules, which aim to guarantee all appliance operations are able to be completed before deadlines. Meanwhile, the power-supply system will not suffer power shortages at different time instants. Before introducing the appliance-level scheduling rule, we first define the maximum energy demanded by an appliance α_i during time period T as $f(\alpha_i, T, t_s)$, which can be calculated by Eq. (8) and Eq. (9) as follows:

$$f(\alpha_i, T, t_s) = P_{\alpha_i}^{max} \cdot \left\lfloor \frac{T}{T_{\alpha_i}} \right\rfloor \cdot L_{\alpha_i} + P_{\alpha_i}^{max} \cdot \max(0, T - \left\lfloor \frac{T}{T_{\alpha_i}} \right\rfloor \cdot T_{\alpha_i} - (T_{\alpha_i} - L_{\alpha_i})) \quad (8)$$

$$f(\alpha_i, T, t_s) = P_{\alpha_i}^{max} \cdot \min(L_{\alpha_i}, t_s + T - t_{\alpha_i}^s, t_{\alpha_i}^s + L_{\alpha_i} - t_s) \quad (9)$$

Given that α_i can be an appliance that releases jobs periodically, such as refrigerator and air-conditioner, it thus can operate multiple times during T . Because jobs of this type of appliances are mostly unshiftable, we separate this calculation into two parts. The first part of Eq. (8) is used to calculate the energy demands of appliance jobs, the duration of which is fully included within the period T starting from time instant t_s , and $\left\lfloor \frac{T}{T_{\alpha_i}} \right\rfloor$ implicitly represents the number of jobs of the appliance α_i during that time period. The second part shows the energy demands of the appliances whose

operating duration is partially included within the period T. Regarding to the appliances that operate sporadically, the energy demands during the period T can be calculated by Eq. (9). The operating duration is the minimum interval length of L_{α_i} , $(t_s + T - t_{\alpha_i}^s)$ and $(t_{\alpha_i}^s + L_{\alpha_i} - t_s)$, where $t_{\alpha_i}^s$ is the start time for α_i to operate, and formally we use the latest start time. In addition, we use $P_{\alpha_i}^{max}$ as the power consumption at each time instant in both Eq. (8) and Eq. (9), the maximum energy demands can thus be obtained.

Based on Eq. (8) and Eq. (9), the appliance-level scheduling rule can be defined as follows:

$$\chi_{\alpha_k} = \frac{\sum_{\alpha_i \in Q_{\alpha}^T} f(\alpha_i, T_{\alpha_k} - L_{\alpha_k} + \sigma, t_{\alpha_k}^r)}{\int_{t_{\alpha_k}^r}^{t_{\alpha_k}^l + \sigma} \left[\sum_{\psi_i \in \psi} P_{\psi_i}^{max}(t) + P_d^{max} - P_{\alpha_k}^{max} + \xi \right] dt} \quad (10)$$

$$t_{\alpha_k}^l = t_{\alpha_k}^r + T_{\alpha_k} - L_{\alpha_k} \quad (11)$$

where $\alpha_k \in \alpha$ denotes the appliance in need of deadline guarantee analysis, $t_{\alpha_k}^r$ represents the release time of the job produced from appliance α_k , $t_{\alpha_k}^l$ denotes its latest start time which can be calculated by Eq. (11), Q_{α}^T is a set of appliances that are powered by renewable energy and operate during the time period T from $t_{\alpha_k}^r$ to $(t_{\alpha_k}^l + \sigma)$, σ is the smallest time unit, the same as the definition in constraint (6), and ξ represents the smallest power unit. For this appliance-level scheduling rule shown in Eq. (10), the numerator part of the fraction on the right hand side is able to calculate maximum renewable energy demands from running appliances except for α_k from $t_{\alpha_k}^r$ to $(t_{\alpha_k}^l + \sigma)$, and the denominator part is used to calculate the minimum renewable energy demands from other appliances that exactly prevent α_k from starting its operation. On the left hand side of Eq. (10), χ_{α_k} refers to the ratio of these two parts, which is a metric responsible for estimating the complexity of finishing job α_k without experiencing operation delay. The larger value of χ_{α_k} indicates more difficulties for appliance α_k to complete the job before the deadline only using power from renewable energy sources.

To avoid operation delay for the appliance α_k , the start time of its job should be strictly no later than $t_{\alpha_k}^l$. Thus we need to check if there is time instant within the period from $t_{\alpha_k}^r$ to $t_{\alpha_k}^l + \sigma$ for α_k to start its job effectively. We always consider the worst case where each appliance $\alpha_i \in Q_{\alpha}^T$ draws maximum energy from renewable energy sources during duration $(T_{\alpha_k} - L_{\alpha_k} + \sigma)$. Therefore, only if $\chi_{\alpha_k} < 1$ is satisfied, implying that sufficient energy generation from renewable energy sources can surely power α_k , α_k is able to start its operation before $t_{\alpha_k}^l$. However, if $\chi_{\alpha_k} \geq 1$, α_k will not guarantee to complete the job before the deadline.

The appliance-level scheduling rule only guarantees that any appliance powered by renewable energy can operate before the latest start time of a particular job, but it cannot guarantee that power generation is sufficient to complete all operations. Thus, the system-level scheduling rule is introduced to avoid power shortage during the operation time of each appliance. We define this rule as Eq. (12):

$$\sum_{\psi_i \in \psi} f(\psi_i, \Gamma, t_0) \geq \sum_{\alpha_i \in Q_{run}^{\Gamma}} f(\alpha_i, \Gamma, t_0) + f(\alpha_k, \Gamma, t_0) \quad (12)$$

$$f(\psi_i, \Gamma, t_0) = \int_{t_0}^{t_0 + \Gamma} P_{\psi_i}^{max}(t) dt + E(t_0) \quad (13)$$

where Γ is the least common multiple of maximum tolerant operating duration T_{α_j} , $\alpha_j \in Q_{run}^{\Gamma} \cup \{\alpha_k\}$, Q_{run}^{Γ} contains jobs that start execution before a new job of α_k but their operation time partially overlaps with the job of α_k , t_0 denotes the earliest start time of α_i , $\alpha_i \in Q_{run}^{\Gamma}$. The total energy demanded by appliances contained in $Q_{run}^{\Gamma} \cup \{\alpha_k\}$ can be

573 calculated by using Eq. (8) and Eq. (9). Eq. (13) is used to calculate the sum of available energy from renewable energy
 574 sources. Only if inequality Eq. (12) is satisfied, entire operations within the lifecycle of a particular job from appliance
 575 α_k can be feasibly accomplished without suffering power shortage.
 576

577 5.2 Allocation Strategy for Appliance Jobs

579 On the basis of the critical scheduling rules presented above, we propose two algorithms which contribute to achieve
 580 maximum utilization of renewable energy in household scenarios. The first algorithm is to initially allocate released
 581 jobs of all smart appliances to an appropriate queue for further scheduling. The pseudo code is shown in Algorithm 1.
 582

583 Algorithm 1 Job Allocation

```

585 1: Initialize: Set up priority queues:
586    $Q_{release} Q_{ready}^r Q_{ready}^g Q_{run}^r Q_{run}^g$ ;
587 2: Assign each queue with value of  $\emptyset$ 
588 3: The following operations will be performed once any appliance releases new job
589 4: for each  $\lambda_{\alpha_k}$  released at time  $t$  do
590 5:    $Q_{release} \leftarrow Q_{release} \cup \{\lambda_{\alpha_k}\}$ 
591 6: end for
592 7: Sort  $Q_{release}$  according to the value of  $\chi$ 
593 8: for each  $\lambda_{\alpha_k} \in Q_{release}$  (with largest  $\chi_{\alpha_k}$  selected first) do
594 9:   if  $f(\alpha_k, \Gamma, t_0)$  meets rule (12) then
595 10:    if  $\chi_{\alpha_k} < 1$  then
596 11:      $Q_{ready}^r \leftarrow Q_{ready}^r \cup \{\lambda_{\alpha_k}\}$  (any insertion for  $Q_{ready}^r$  and  $Q_{ready}^g$  are according to the usage priority)
597 12:     for each  $\alpha_i \in Q_{ready}^r$  do
598 13:       if  $\chi_{\alpha_i} \geq 1$  or inequality (12) is not satisfied then
599 14:          $Q_{ready}^g \leftarrow Q_{ready}^g \cup \{\lambda_{\alpha_k}\}$ 
600 15:          $Q_{ready}^r \leftarrow Q_{ready}^r \setminus \{\lambda_{\alpha_k}\}$ 
601 16:       end if
602 17:     end for
603 18:   else
604 19:      $Q_{ready}^g \leftarrow Q_{ready}^g \cup \{\lambda_{\alpha_k}\}$ 
605 20:   end if
606 21: else
607 22:    $Q_{ready}^g \leftarrow Q_{ready}^g \cup \{\lambda_{\alpha_k}\}$ 
608 23: end if
609 24: end for

```

613 In Algorithm 1, λ_{α_k} denotes a particular job of the appliance α_k . Initially, Lines 1-2 set up five queues. $Q_{release}$ is
 614 used to contain the jobs to be finished released by appliances. Two ready queues Q_{ready}^r and Q_{ready}^g are comprised
 615 of appliances which are ready to operate and powered by two different energy sources, namely renewable energy
 616 and energy from utility grid. Another two running queues Q_{run}^r and Q_{run}^g contain the currently-running appliances
 617 powered by these two energy sources. Once any appliance releases a job, it will be first allocated to $Q_{release}$ and then
 618 this queue will be sorted based on χ of each appliance in the $Q_{release}$, which is presented in lines 4-7. Lines 8-22 are
 619 used to filter out the appliances completely powered by renewable energy based on the appliance-level and system-level
 620 scheduling rules, and insert these appliance jobs into Q_{ready}^r based on different usage priorities which corresponds to
 621 the deadlines. As mentioned before, the earlier deadline a job has, the higher priority it is assigned. Therefore, this
 622

allocation method implicitly ensures that the job with higher priority in Q_{ready}^r will be executed earlier, which not only simplifies the work in the following scheduling stage, but also significantly lowers the risk of sacrificing users' comfort. Once the job newly inserted in Q_{ready}^r is assigned with higher priority than some existing jobs in the same queue, the execution order of these jobs would be adjusted, leading to the deadline violation. To avoid this case, the system needs to individually check the satisfaction of the appliance-level scheduling rule for all these jobs as shown in Lines 12-17. For other appliances violating these two scheduling rules, the system will put them into Q_{ready}^g .

5.3 Scheduling Strategy for Appliance Jobs on Q_{ready}^r

Algorithm 2 Job Scheduling on Q_{ready}^r

```

1: while System is on do
2:   for each  $\lambda_{\alpha_k} \in Q_{ready}^r$  (with high priority selected first) do
3:     if  $p_{\alpha_k}^{max} < \sum_{\psi_i \in \psi} p_{\psi_i}^{max}(t) + p_d^{max} - \sum_{\alpha_i \in Q_{run}^r} p_{\alpha_i}^{max}$  then
4:       Search for  $\omega_{\alpha_k}^{\zeta} \in \omega_{\alpha_k}$  corresponding to users preference
5:       Search for a working mode  $m_{\alpha_k}^{\zeta} \in m_{\alpha_k}$  mapping to  $\omega_{\alpha_k}^{\zeta}$ 
6:        $Q_{run}^r \leftarrow Q_{run}^r \cup \lambda_{\alpha_k}$ 
7:        $Q_{ready}^r \leftarrow Q_{ready}^r \setminus \lambda_{\alpha_k}$ 
8:       for each  $\lambda_{\alpha_i} \in Q_{ready}^r$  do
9:         if  $\chi_{\alpha_i} \geq 1$  or inequality (12) is not satisfied then
10:           $Q_{ready}^g \leftarrow Q_{ready}^g \cup \{\lambda_{\alpha_i}\}$ 
11:           $Q_{ready}^r \leftarrow Q_{ready}^r \setminus \{\lambda_{\alpha_i}\}$ 
12:        end if
13:      end for
14:    end if
15:  end for
16:  The following steps will be executed only if any appliance finishes its job
17:  for each  $\lambda_{\alpha_j}$  finished at time t do
18:    if  $\lambda_{\alpha_j} \in Q_{run}^r$  then
19:       $Q_{run}^r \leftarrow Q_{run}^r \setminus \{\lambda_{\alpha_j}\}$ 
20:    else
21:       $Q_{run}^g \leftarrow Q_{run}^g \setminus \{\lambda_{\alpha_j}\}$ 
22:    end if
23:  end for
24: end while

```

After selecting the appropriate power source for each released appliance job, the system is supposed to realize online scheduling on Q_{ready}^r and Q_{ready}^g . Algorithm 2 presents the detailed procedure of performing job scheduling on Q_{ready}^r . To maximize the utilization of renewable energy, the difference between total renewable energy generation and total energy consumption of appliance jobs from the running queue is taken into account. When the energy generation is greater than the maximum power consumption of an appliance α_k , the new job λ_{α_k} will be added to the running queue and the appliance will start its operations immediately, as depicted in lines 3-7. In this procedure, if the selected appliance is an adjustable one, it needs to be set to an appropriate working mode which not only reduces energy drawn from utility grid, but also meets users' preferences. Considering cases where appliance jobs with lower priority may be executed first only if the requirement shown in line 3 is satisfied, the actual operation sequence of the appliances in

677 Q_{ready}^r would be changed accordingly. Thus, the system is required to check the appliance-level scheduling rule for
 678 each appliance in Q_{ready}^r once a new job is added into Q_{run}^r in case of causing operation delay. Once the appliance
 679 finishes all operations of a job, the job is removed from the running queue as depicted in lines 16-23.
 680
 681

682 **Algorithm 3** Job Scheduling on Q_{ready}^g

683
 684
 685 1: The following operations will be performed once new appliance job is inserted into Q_{ready}^g
 686
 687 2: Search for $\omega_{\alpha_k}^\zeta \in \omega_{\alpha_k}$ corresponding to users preference
 688 3: Search for a working mode $m_{\alpha_k}^\zeta \in m_{\alpha_k}$ mapping to $\omega_{\alpha_k}^\zeta$
 689 4: Search for a working power $\rho_{\alpha_k}^\zeta \in \rho_{\alpha_k}$ mapping to $m_{\alpha_k}^\zeta$
 690 5: $\lambda_{first} \leftarrow Q_{ready}^g[0]$
 691 6: $\lambda_{last} \leftarrow Q_{ready}^g[n]$
 692 7: $\tau_0 \leftarrow t_{\alpha_{first}}^r$
 693 8: $\tau_n \leftarrow t_{\alpha_{last}}^r + T_{\alpha_{last}}$
 694 9: $F(\tau_0, s(\tau_0)) = 0$
 695 10: **for** $\tau_i = \tau_0$ **to** τ_n **do**
 696 11: **for** each possible system state $s(\tau_i)$ at τ_i **do**
 697 12: **for** each $\lambda_{\alpha_k} \in Q_{ready}^g$ **do**
 698 13: **if** $t_{\alpha_k}^r \leq \tau_i \leq (t_{\alpha_k}^r + T_{\alpha_k} - L_{\alpha_k})$ **then**
 699 14: **if** $\tau_i \leq (t_{\alpha_k}^r + T_{\alpha_k} - L_{\alpha_k}) \leq \tau_{i+1}$ **then**
 700 15: $Q_{run}^g \leftarrow Q_{run}^g \cup \{\lambda_{\alpha_k}\}$ (not real scheduling)
 701 16: $Q_{ready}^g \leftarrow Q_{ready}^g \setminus \{\lambda_{\alpha_k}\}$ (not real scheduling)
 702 17: **else**
 703 18: Add λ_{α_k} into the job set $\Lambda[]$ as a candidate
 704 19: **end if**
 705 20: **end if**
 706 21: **end for**
 707 22: Calculate all possible subsets of $\Lambda[]$
 708 23: **for** each possible job set $\phi \subset \Lambda$ **do**
 709 24: **for** each $\lambda_{\alpha_j} \in \phi$ **do**
 710 25: **if** $(\sum_{\lambda_{\alpha_i} \in Q_{run}^g} p_{\alpha_i}^{max} + p_{\alpha_k}^{max}) \leq p_{grid}^{max}$ **then**
 711 26: $Q_{run}^g \leftarrow Q_{run}^g \cup \{\lambda_{\alpha_j}\}$ (not real scheduling)
 712 27: $Q_{ready}^g \leftarrow Q_{ready}^g \setminus \{\lambda_{\alpha_j}\}$ (not real scheduling)
 713 28: **end if**
 714 29: **end for**
 715 30: **end for**
 716 31: **end for**
 717 32: Gain all possible system states $S(\tau_{i+1})$ at τ_{i+1} after above operations
 718 33: **for** each possible system state $s(\tau_{i+1})$ at τ_{i+1} **do**
 719 34: $F(\tau_{i+1}, s(\tau_{i+1})) \leftarrow \min\{F(\tau_i, s(\tau_i)) + W(s(\tau_i), s(\tau_{i+1}))\}$;
 720 35: **end for**
 721 36: **end for**
 722 37: Schedule the jobs in Q_{ready}^g based on critical path reaching to $s(\tau_n)$
 723
 724
 725
 726
 727
 728

5.4 Scheduling Strategy for Appliance Jobs on Q_{ready}^g

For the appliance jobs assigned to Q_{ready}^g , we also develop an optimal scheduling strategy, which can substantially reduce the energy cost for each household. Before getting into the details of the algorithm, we first model the scheduling problem as follows.

$$\min \left\{ \sum_{\lambda_{\alpha_i} \in Q_{ready}^g} \left[\int_{t_{\alpha_i}^s}^{t_{\alpha_i}^s + T_{\alpha_i}} C_{grid}(t) \cdot P_{\alpha_i}(t) dt \right] \right\} \quad (14)$$

subject to

$$t_{\alpha_i}^r \leq t_{\alpha_i}^s \leq (t_{\alpha_i}^r + L_{\alpha_i} - T_{\alpha_i}), \forall \alpha_i \in Q_{ready}^g \quad (15)$$

$$\sum_{\lambda_{\alpha_i} \in Q_{ready}^g} P_{\alpha_i}(t) \leq P_{grid}^{max} \quad (16)$$

As shown in (14), the objective of the scheduling is to minimize the total energy cost of the jobs currently within Q_{ready}^g . $t_{\alpha_i}^s$ denotes the start time of a certain appliance job λ_{α_i} , which is a decision variable in this optimization problem. Thus the number of decision variables is equal to the number of appliance jobs within Q_{ready}^g . Meanwhile, there are two critical constraints (15) and (16) as basic scheduling principles that the system should satisfy when deriving job schedules. The employment of constraint (15) guarantees that each job is able to finish its entire operations no later than its deadline, and the constraint (16) indicates that total power consumption at a given time instant cannot exceed a certain power bound which depends on the power capability of the utility grid. In an effort to derive cost-effective schedules for the whole system, we developed a dynamic programming (DP) based strategy in Algorithm 3.

In Algorithm 3, $S(\tau_i)$ denotes a set of possible system states at time instant τ_i , and $s(\tau_i)$ is one of the elements within that set, recording the state of each job either in Q_{run}^g or Q_{ready}^g . $F(\tau_i, s(\tau_i))$ is the cost-to-go for this system when the DP algorithm is employed, which represents minimum total energy cost to reach system state $s(\tau_i)$ from the beginning of runtime, and $W(s(\tau_i), s(\tau_{i+1}))$ denotes the optimal transition cost from $s(\tau_i)$ to $s(\tau_{i+1})$, which is used to calculate $F(\tau_{i+1}, s(\tau_{i+1}))$. The entire procedure in Algorithm 3 will only be performed once a new appliance job is inserted into Q_{ready}^g . In the procedure, we firstly identify the operating duration of appliance jobs, starting from the release time of the first job and ending at the deadline of the last job within Q_{ready}^g . We also select the appropriate working mode for the appliances that have job(s) currently allocated in the Q_{ready}^g as shown in lines 2-4, which aims to reduce energy consumption while guaranteeing performance satisfaction. Then, the system is expected to iteratively search for cost-effective schedules at different stages. As depicted in lines 11-31, based on constraints 15 and 16, the system will filter out a set of appliance jobs $\Lambda[\]$ that could be added into Q_{run}^g at certain stage τ_i and search for all possible system states at τ_{i+1} by dispatching different combinations of candidate appliance jobs into Q_{run}^g . For each possible system state at τ_{i+1} , optimal energy cost can be calculated by employing the formula shown in line 34. Ultimately, minimum total energy cost at the final state $s(\tau_n)$ can be calculated and the optimal job schedules at different stages are effectively generated as well.

6 A PROOF-OF-CONCEPT CASE STUDY

To evaluate the feasibility and the performance of our design, we set up a small-scale testbed powered by a hybrid energy supply, which includes renewable energy generators and the utility grid. In this testbed, we used real-world

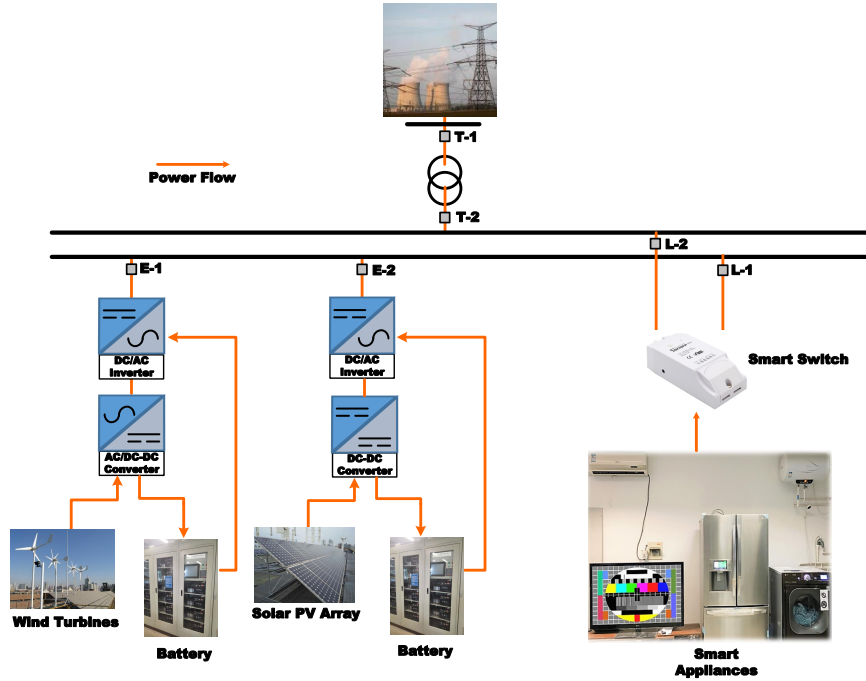


Fig. 2. Experiment Setup

smart appliances to emulate a household scenario. In this section, we firstly introduce the details of our experiment setup and the implementation of our proposed framework. Then the results of the performance evaluation will be discussed.

6.1 Experiment Setup

In this experiment, we designed a testbed as shown in Fig. 2, which can be deemed as a household. The smart appliances used in this testbed include smart refrigerator, washing machine, air-conditioner, TV and water heater. The average power consumption of a TV is 100W and the air-conditioner consumes 665W in an hour. For the washing machine, two washing programs were considered in this experiment, which are daily wash (137W) and delicate (147W) respectively. The smart refrigerator can also work in two different modes, which on average consume 98W and 78W respectively. Regarding the water heater, we selected three setpoints, 60°C, 65°C and 70°C, any of which is possible to be set in our daily life. Based on a long-term measurement, we figured out that the average power consumption of these three setpoints are 1216W, 1330W and 1551W respectively. A Raspberry Pi 3B device with a quad-core CPU and 1 GB RAM was used for running our proposed framework. In addition, this testbed was equipped with multiple smart switches to remotely control the running of corresponding appliances and adjust their working modes. To store the surplus energy from the renewable energy source, we used a Lithium-ion battery with capacity of 1.5KWh in our experiments.

In this testbed, a hybrid power supply system was employed to power these smart appliances, which combines renewable energy generators and utility grid. To generate renewable energy, we set up photovoltaic arrays as a solar energy source and three wind turbines as a wind power source. The photovoltaic arrays have peak output power of 600W

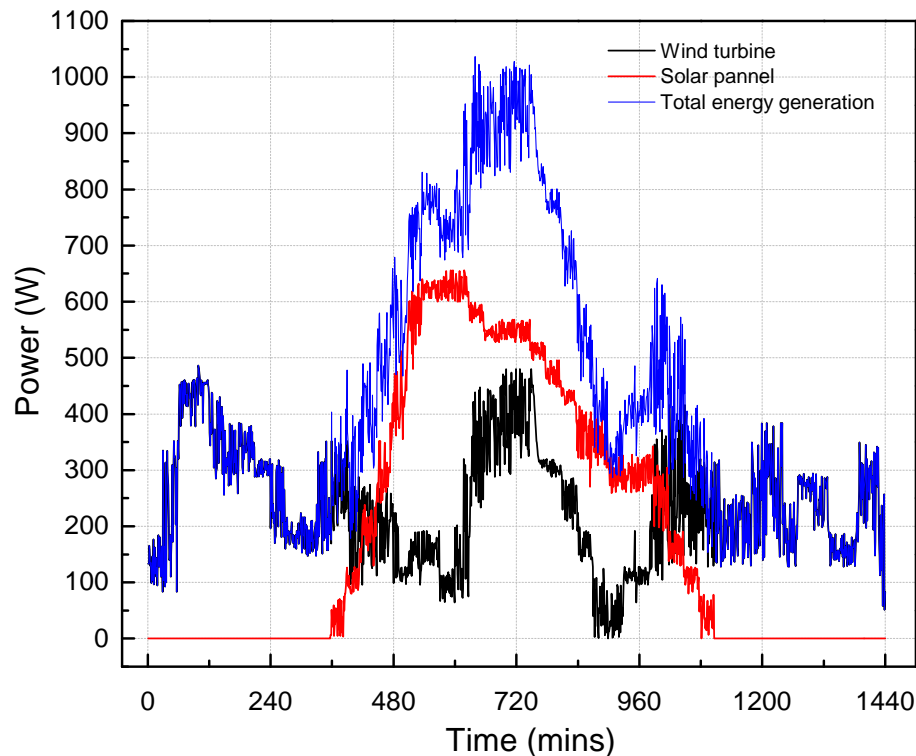


Fig. 3. Power Generation

Table 2. Energy Consumption

Experimental case	Renewable energy generation	Total energy consumption	Renewable energy consumption
Case 1	10.03KWh	6.75KWh	3.15KWh
Case 2	10.03KWh	6.38KWh	4.79KWh

and the peak power output of each wind turbine can be 150W. To enhance reliability of the whole system and derive optimal appliance schedules, we conducted intra-day energy generation prediction based on weather forecasts acquired from Solcast [Sol [n. d.]] and Windfinder [Win [n. d.]]. Both of them provide API for users to retrieve forecasting information of sunlight intensity, temperature, wind gusts and wind speed from a given location. As is well known, day-ahead pricing information is supposed to be periodically retrieved from the utility company. In Australia, the electricity prices over a day that residential users get from energy retailers are three static values, matching up with three fixed time periods, peak hours, off-peak hours and shoulder hours respectively. With respect to aggregated energy consumption, we used one smart meter measuring energy consumption of all appliances, and then derived fine-grained appliance-level information by using the NILM algorithm employed in one of our previous works.

To benchmark the performance of our design, we also conducted experiments without any schedule strategies on each appliance, simply aligning with users' behavior in daily routine. The results of this experiment will be compared with the case employing the proposed scheduling strategies.

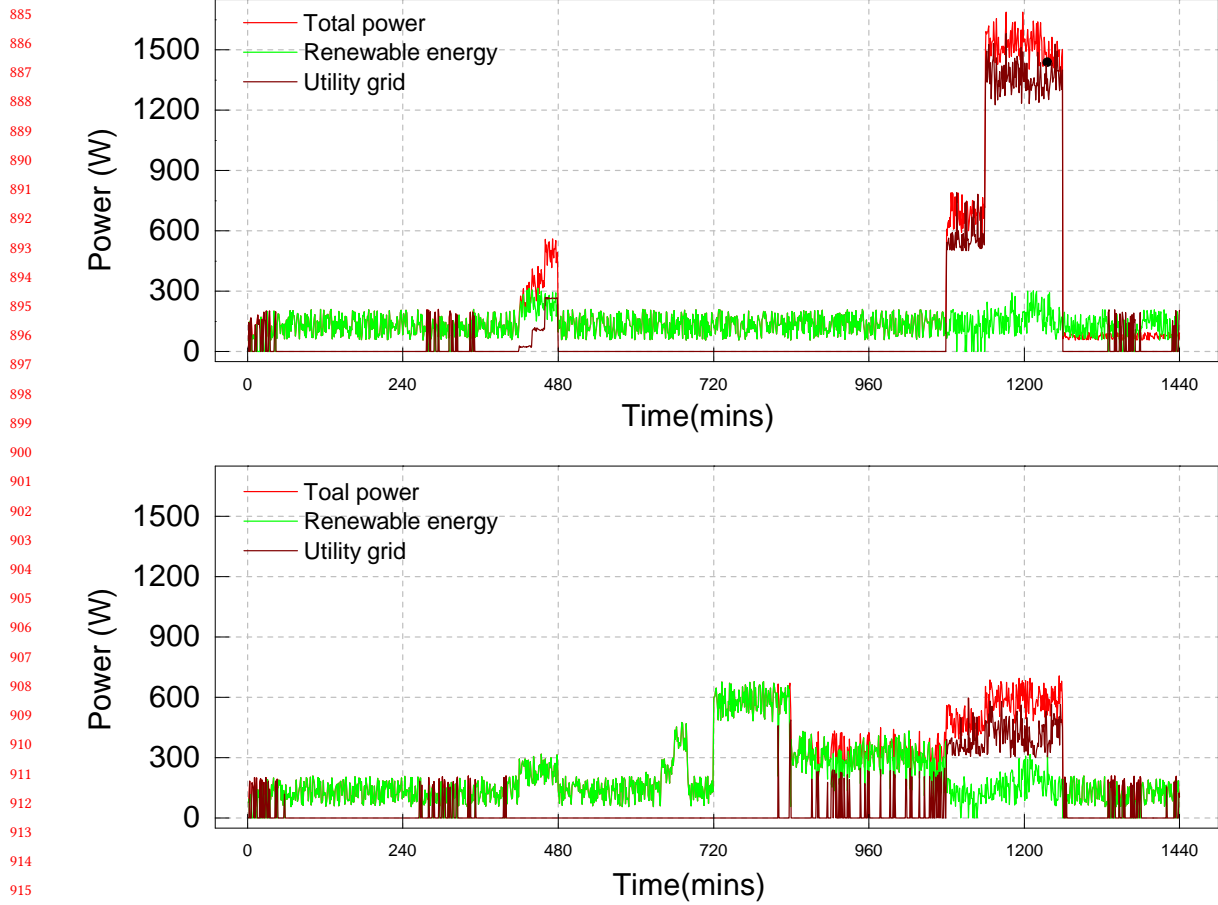


Fig. 4. Power Consumption

6.2 Performance Evaluation

We evaluated the performance of our proposed HilCPS-based energy management system over five weekdays and collected corresponding data. Fig. 3 shows the renewable energy generation on one day. The largest proportion of renewable energy generation comes from 9AM to 4PM and the peak output power of this solar-wind hybrid power supply can reach to 1020W at around 1PM. Actual energy consumption from both renewable energy sources and utility grid are shown in Fig. 4. In this experiment, we compared renewable energy usage between two experimental cases realized by two different scheduling strategies.

As shown in the upper part of Fig. 4, we emulated the daily routine of a typical family and the appliances ran immediately once the jobs were released, without employing any scheduling strategies. The schedule profile generated from the appliance control module was based on residential habits in a typical day. Within the selected day, the smart refrigerator mostly drew energy from renewable energy sources except for the period 0AM-1AM and 6AM-7AM. During the daytime from 6AM to 5PM, most energy consumption was covered by renewable energy, and the surplus energy generated from photovoltaic arrays and wind turbines was stored in batteries for future use. However, from 7AM to 8AM, renewable energy was not sufficient to support the running of the washing machine, thus it fully drew power

937 from utility grid during that time period. From 6PM to 9PM, as user activities significantly increased, a set of appliances
938 was turned on, including air-conditioner, TV and water heater. The available renewable energy was not sufficient in that
939 time period, and the energy stored in the battery was quickly depleted by 7PM. The energy consumed by appliances
940 is mainly supplied by utility grid. In this case, as shown in Table 2, the sum of energy consumption is 6.75KWh and
941 renewable energy generators produced 10.03KWh energy in total. Only 3.15KWh renewable energy, however, was
942 consumed by the appliances, which represents 46% of total energy consumption. Thus, only 30% of total renewable
943 energy generation was used, but more renewable energy was wasted.
944

945 The bottom part of Fig. 4 shows the energy consumption of appliances that followed the schedule strategies
946 proposed in the last section. In this experiment, the appliances are firstly classified into two types, shiftable appliances
947 and unshiftable appliances. The unshiftable appliances, including TV, air conditioner, and refrigerator, need to run
948 immediately once the jobs were released. In contrast, the shiftable appliances deployed in our testbed, including washing
949 machine and water heater, are more flexible to adjust their operation time. Therefore, the operation time of both
950 appliances could be arranged to work during the period when the renewable energy supply was plentiful. To meet the
951 deadlines of the jobs, as shown in Fig. 4, the washing machine was scheduled to operate from 9AM to 10AM, and water
952 heater started working at 1PM and finished the job before 9PM. By doing so, the deadline of each appliance job was
953 thus guaranteed. In addition, the battery was fully charged by 5PM before the solar energy generation dropped down to
954 zero. Since most workloads of appliances are shifted to daytime, the energy demands at peak hours were significantly
955 alleviated. From 6PM to 9PM, most energy supply from utility grid was drawn by the air-conditioner due to its low
956 flexibility. The remaining workload could be fully powered by the battery and the renewable energy generated from
957 wind turbines until 10PM, exactly avoiding the peak hours. In this experiment, because the water heater and washing
958 machine were adjusted to a relatively low working mode based on user preferences, total energy consumption dropped
959 down to 6.38KWh. As shown in Table 2, the total renewable energy usage reached 4.79KWh, which takes up to 48%
960 of total renewable energy generation and 75% of total energy consumption. Compared to the previous experiment,
961 this experiment employing the effective online scheduling strategies not only shows significant improvement on the
962 utilization of renewable energy, but also shows high reduction of energy demands.
963

964 6.3 Cost Reduction

965 To study the cost reduction when the proposed scheduling strategies are employed, we analyzed the distribution of
966 appliance loads in two different experimental cases during the selected day, which were powered by utility grid. As
967 shown in the upper part of Fig. 5, the blue line represents the variation of the real-time electricity price within a day. In
968 Australia, the electricity market is operated by the Australian Energy Market Operator, which offers electricity to the
969 energy retailers at every five minute interval with the average price over the past 30 minutes. As shown in Fig. 5, most
970 energy consumption occurred at the peak hours (6PM-9PM) when the electricity price was high, leading to high energy
971 cost. In the bottom part of Fig. 5, partial workloads from appliances were shifted to the period from 3PM to 6PM when
972 the electricity price was lower. Furthermore, every appliance was adjusted to a lower setpoint or working mode without
973 jeopardizing users' comfort. Comparing these two different cases, the energy cost was significantly reduced by 60%.
974

975 7 CONCLUSION

976 We propose a HilCPS based energy management system in this article, which explicitly take human interactions into
977 consideration to guarantee the needs of users are fully met. In this system, we support analysis of user preference on
978 each appliance and use an entropy-based solution to convert the flexibility of appliances into deadlines. Moreover, on
979

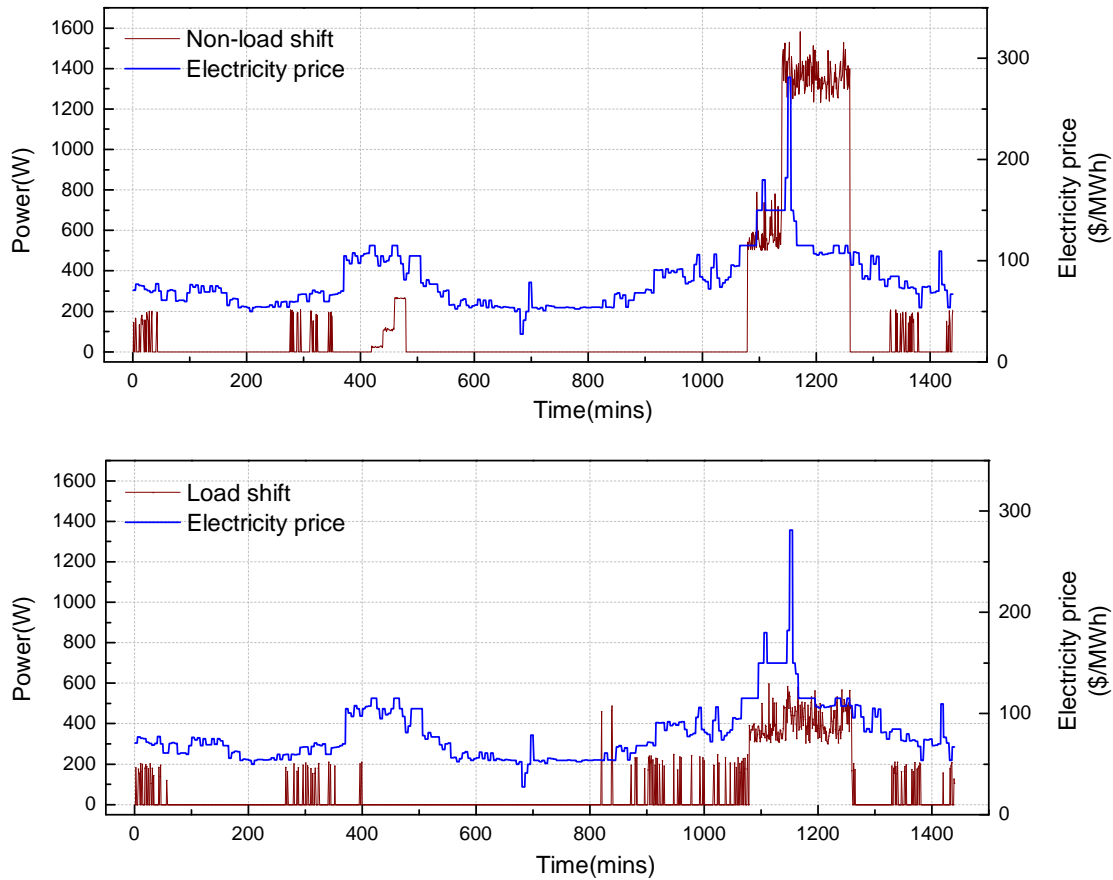


Fig. 5. Cost Reduction

top of a traditional load shifting approach, an optimal scheduling strategy for appliance jobs is presented, which is helpful to achieve energy management in a sustainable way without jeopardizing users' comfort. To conduct evaluation of this system framework and proposed scheduling strategy, we implement a testbed with real smart appliances, and practically prove that this system can effectively maximize the utilization of local renewable energy and significantly lower energy cost.

REFERENCES

- [n. d.]. Renewable energy: A world turned upside down, The Economist. <http://www.economist.com/news/briefing/21717365-wind-and-solar-energy-are-disrupting-century-old-model-providing-electricity-what-will>. Accessed: 2017-08-17.
- [n. d.]. Solcast. <https://solcast.com.au>. Accessed: 2018-03-25.
- [n. d.]. Windfinder. <https://www.windfinder.com/weather-maps/forecast/>. Accessed: 2018-04-20.
- Baris Aksanli and Tajana S Rosing. 2017. Human behavior aware energy management in residential cyber-physical systems. *IEEE Transactions on Emerging Topics in Computing* (2017).
- Pietro Cottone, Salvatore Gaglio, Giuseppe Lo Re, and Marco Ortolani. 2015. User activity recognition for energy saving in smart homes. *Pervasive and Mobile Computing* 16 (2015), 156 – 170. <https://doi.org/10.1016/j.pmcj.2014.08.006>
- Erdem Cuce, Pinar Mert Cuce, and Tulin Bali. 2013. An experimental analysis of illumination intensity and temperature dependency of photovoltaic cell parameters. *Applied Energy* 111 (2013), 374–382.

- 1041 Elham Delzendeh, Song Wu, Angela Lee, and Ying Zhou. 2017. The impact of occupants' behaviours on building energy analysis: A research review.
1042 *Renewable and Sustainable Energy Reviews* 80 (2017), 1061 – 1071. <https://doi.org/10.1016/j.rser.2017.05.264>
- 1043 Suman Giri and Mario Bergés. 2015. An energy estimation framework for event-based methods in Non-Intrusive Load Monitoring. *Energy Conversion and*
1044 *Management* 90 (2015), 488–498.
- 1045 Sayed Saeed Hosseini, Kodjo Agbossou, Sousso Kelouwani, and Alben Cardenas. 2017. Non-intrusive load monitoring through home energy management
1046 systems: A comprehensive review. *Renewable and Sustainable Energy Reviews* 79 (2017), 1266–1274.
- 1047 Branislav Hredzak, Vassilios G Agelidis, and Minsoo Jang. 2014. A model predictive control system for a hybrid battery-ultracapacitor power source. *IEEE*
1048 *Transactions on Power Electronics* 29, 3 (2014), 1469–1479.
- 1049 Azim Keshthkar and Siamak Arzanpour. 2017. An adaptive fuzzy logic system for residential energy management in smart grid environments. *Applied*
1050 *Energy* 186 (2017), 68 – 81. <https://doi.org/10.1016/j.apenergy.2016.11.028>
- 1051 S. Lee, G. Ryu, Y. Chon, R. Ha, and H. Cha. 2013. Automatic Standby Power Management Using Usage Profiling and Prediction. *IEEE Transactions on*
1052 *Human-Machine Systems* 43, 6 (Nov 2013), 535–546. <https://doi.org/10.1109/THMS.2013.2285921>
- 1053 W. Li, T. Yang, F. C. Delicato, P. F. Pires, Z. Tari, S. U. Khan, and A. Y. Zomaya. 2018. On Enabling Sustainable Edge Computing with Renewable Energy
1054 Resources. *IEEE Communications Magazine* 56, 5 (May 2018), 94–101. <https://doi.org/10.1109/MCOM.2018.1700888>
- 1055 Jacob Mattingley, Yang Wang, and Stephen Boyd. 2011. Receding horizon control. *IEEE Control Systems* 31, 3 (2011), 52–65.
- 1056 Matteo Muratori, Matthew C. Roberts, Ramteen Sioshansi, Vincenzo Marano, and Giorgio Rizzoni. 2013. A highly resolved modeling technique to simulate
1057 residential power demand. *Applied Energy* 107 (2013), 465 – 473. <https://doi.org/10.1016/j.apenergy.2013.02.057>
- 1058 D. S. Nunes, P. Zhang, and J. S. Silva. 2015. A Survey on Human-in-the-Loop Applications Towards an Internet of All. *IEEE Communications Surveys*
1059 *Tutorials* 17, 2 (Secondquarter 2015), 944–965. <https://doi.org/10.1109/COMST.2015.2398816>
- 1060 G. Schirmer, D. Erdogmus, K. Chowdhury, and T. Padir. 2013. The Future of Human-in-the-Loop Cyber-Physical Systems. *Computer* 46, 1 (Jan 2013),
1061 36–45. <https://doi.org/10.1109/MC.2013.31>
- 1062 Akshay SN Uttama Nambi, Antonio Reyes Lua, and Venkatesha R Prasad. 2015. Loded: Location-aware energy disaggregation framework. In *Proceedings*
1063 *of the 2nd ACM International Conference on Embedded Systems for Energy-Efficient Built Environments*. ACM, 45–54.
- 1064 J. Venkatesh, B. Aksanli, J. Junqua, P. Morin, and T. S. Rosing. 2013. HomeSim: Comprehensive, smart, residential electrical energy simulation and
1065 scheduling. In *2013 International Green Computing Conference Proceedings*. 1–8. <https://doi.org/10.1109/IGCC.2013.6604479>
- 1066 Rongxin Yin, Emre C. Kara, Yaping Li, Nicholas DeForest, Ke Wang, Taiyou Yong, and Michael Stadler. 2016. Quantifying flexibility of commercial and
1067 residential loads for demand response using setpoint changes. *Applied Energy* 177 (2016), 149 – 164. <https://doi.org/10.1016/j.apenergy.2016.05.090>
- 1068 S. Zhai, Z. Wang, X. Yan, and G. He. 2018. Appliance Flexibility Analysis Considering User's Behavior in Home Energy Management System Using Smart
1069 Plugs. *IEEE Transactions on Industrial Electronics* (2018), 1–1. <https://doi.org/10.1109/TIE.2018.2815949>
- 1070 Bin Zhou, Wentao Li, Ka Wing Chan, Yijia Cao, Yonghong Kuang, Xi Liu, and Xiong Wang. 2016. Smart home energy management systems: Concept,
1071 configurations, and scheduling strategies. *Renewable and Sustainable Energy Reviews* 61 (2016), 30 – 40. <https://doi.org/10.1016/j.rser.2016.03.047>
- 1072
- 1073
- 1074
- 1075
- 1076
- 1077
- 1078
- 1079
- 1080
- 1081
- 1082
- 1083
- 1084
- 1085
- 1086
- 1087
- 1088
- 1089
- 1090
- 1091
- 1092